STEM CELLS AND DEVELOPMENT
Volume 26, Number 23, 2017
Mary Ann Liebert, Inc.
DOI: 10.1089/scd.2017.0172

Drug-Mediated Shortening of Action Potentials in LQTS2 Human Induced Pluripotent Stem Cell-Derived Cardiomyocytes

Gary Duncan,[1] Karl Firth,[1] Vinoj George,[1,2] Minh Duc Hoang,[1,2] Andrew Staniforth,[3] Godfrey Smith,[4] and Chris Denning[1]

Cardiomyocytes (CMs) derived from human induced pluripotent stem cells (hiPSCs) are now a well-established modality for modeling genetic disorders of the heart. This is especially so for long QT syndrome (LQTS), which is caused by perturbation of ion channel function, and can lead to fainting, malignant arrhythmias and sudden cardiac death. LQTS2 is caused by mutations in *KCNH2*, a gene whose protein product contributes to I_{Kr} (also known as HERG), which is the predominant repolarizing potassium current in CMs. β-blockers are the mainstay treatment for patients with LQTS, functioning by reducing heart rate and arrhythmogenesis. However, they are not effective in around a quarter of LQTS2 patients, in part, because they do not correct the defining feature of the condition, which is excessively prolonged QT interval. Since new therapeutics are needed, in this report, we biopsied skin fibroblasts from a patient who was both genetically and clinically diagnosed with LQTS2. By producing LQTS-hiPSC-CMs, we assessed the impact of different drugs on action potential duration (APD), which is used as an in vitro surrogate for QT interval. Not surprisingly, the patient's own β-blocker medication, propranolol, had a marginal effect on APD in the LQTS-hiPSC-CMs. However, APD could be significantly reduced by up to 19% with compounds that enhanced the I_{Kr} current by direct channel binding or by indirect mediation through the PPARδ/protein 14-3-3 epsilon/HERG pathway. Drug-induced enhancement of an alternative potassium current, I_{KATP}, also reduced APD by up to 21%. This study demonstrates the utility of LQTS-hiPSC-CMs in evaluating whether drugs can shorten APD and, importantly, shows that PPARδ agonists may form a new class of therapeutics for this condition.

Keywords: human induced pluripotent stem cells, cardiomyocytes, long QT syndrome, electrophysiology, HERG, PPAR delta

Introduction

Long QT Syndrome (LQTS) is a genetic heart abnormality characterized by extended duration of the QT interval on an electrocardiogram. A corrected QT (QTc) that exceeds 450 ms in males and 460 ms in females is considered prolonged [1]. Symptoms of LQTS can include a repeated history of fainting and *Torsade-de-Pointes*, a form of polymorphic ventricular tachycardia that can lead to ventricular fibrillation and sudden cardiac death [2]. Early diagnosis of LQTS by clinical and/or genetic evaluation is important because the first presentation may be life threatening [3]. Sudden infant death syndrome affects 1 in 2,000 births, of which 12% are thought to be caused by underlying LQTS [4,5]. Moreover, there is a 21% mortality rate for symptomatic patients who remain untreated for 1 year [4].

Thirteen subtypes of LQTS have been identified, with the most prevalent forms being LQTS1, 2, and 3 [3,4]. LQTS2 accounts for ~35% to 40% of LQTS cases and the underlying cause is mutation of the *KCNH2* gene. This encodes the α-subunit of the rapid-acting inward rectifying potassium I_{Kr} current (also known as HERG or Human Ether-a-go-go-related Gene) and drives rapid repolarization during the cardiac cycle [4]. Diagnosis is often followed by prescription of β-blockers, such as propranolol and nadolol, as the first line of treatment [6]. This approach has proven effective for LQTS1 patients, reducing mortality rate to 0.5%. However, β-blockers may be ineffective in up to 23% of LQTS2 cases [7,8]. These drugs block the proarrhythmic effects of circulating adrenergic agonists and the sympathetic nervous system to cause a slowing in heart rate.

[1]Department of Stem Cell Biology, Centre of Biomolecular Sciences, University of Nottingham, Nottingham, United Kingdom.
[2]Guy Hilton Research Centre, Institute for Science and Technology in Medicine (ISTM), Keele University, Staffordshire, United Kingdom.
[3]Department of Cardiovascular Medicine, Queen's Medical Centre, Nottingham, United Kingdom.
[4]Institute of Cardiovascular and Medical Sciences, University of Glasgow, Glasgow, United Kingdom.

Paradoxically, however, a slower heart rate can be associated with prolonged QT interval. In LQTS patients, where QT interval is already long, patients may need to receive an atrial pacemaker to elevate rate back to normal levels. Therefore, β-blockers do not treat, and can exacerbate, the underlying condition of excessively long QT interval and low rate of cardiac repolarization.

Human induced pluripotent stem cells (hiPSCs), produced by epigenetic reprogramming of somatic cells, can be differentiated into cardiomyocytes (CMs) at high efficiency, which has provided a renewable method to create ''patient in a dish'' models of genetic disease. For channel-based disorders, this includes LQTS types 1 [9], 2 [10], 3 [11], and 8 [12,13], as well as LQTS3/Brugada overlap [13] and catecholaminergic polymorphic ventricular tachycardia [14]. The LQTS models have been used to demonstrate that approved and experimental drugs can be effective in reducing the action potential duration (APD) and arrhythmic events in hiPSC-CMs, suggesting further extension of these studies is warranted. To this end, we sought to evaluate the impact of a panel of seven drugs, including β-blockers, I_{katp} and I_{kr} modulators, and for the first time PPARδ agonists, on APD and repolarization rates in LQTS2-hiPSC-CMs.

Materials and Methods

All culture was at 37°C, 5% CO_2 in a humidified environment. All reagents for hiPSC production and culture were from ThermoFisher unless specified.

Generating hiPSCs

Skin fibroblasts were derived under ethical consent, as previously described [10]. Reprogramming to hiPSCs was done using the CytoTune 2.0 nonintegrating Sendai virus. In brief, on d0, one well of a six-well plate was seeded with 2×10^5 cells in a fibroblast medium (DMEM supplemented with 10% fetal calf serum, 1% nonessential amino acids, 1% glutamine, and 100 μM β-mercaptoethanol). On d1, CytoTune 2.0 was added to 3 mL of fibroblast medium to give an MOI of 5:5:3 and this was used to replace the medium on the cells. From d2 to ~d5, the fibroblast medium was changed daily until the cells reached ~80% confluence. On d5, the cells were passaged using 0.05% trypsin and split at a ratio of 1:3 into 3×35 mm dishes coasted in vitronectin peptide and cultured in E6 medium supplemented with 100 ng/mL of basic fibroblast growth factor (FGF2; PeproTech). The medium was changed daily until the emergence of definitive hiPSC colonies by ~d12, at which point the medium was changed to E8 medium. E8 medium was changed daily until ~d21 when individual colonies were isolated by mechanical dissociation using a stem cell cutting tool (14601; 0.190–0.210 mm; Vitrolife) and seeded into 48-well plates coated in Matrigel for expansion in E8 medium.

Confirming pluripotent phenotype

Transcription factors associated with pluripotency were assessed in hiPSCs by washing phosphate-buffered saline and then fixing in 4% paraformaldehyde for 15 min at room temperature. Permeabilization was with 0.1% Triton X-100 for 10 min. The primary antibodies used were anti-OCT4 (1:50, mouse, SC-5279; Santa Cruz), anti-SOX2 (1:200, goat, AF2018; R&D Systems) and anti-NANOG (1:200, goat, AF1997; R&D Systems), with reactions carried out overnight at 4°C. Alexa-488 conjugated secondary antibodies were used, either as anti-mouse (1:1,000, A32723; Invitrogen) or anti-goat (1:1,000, A11055; Invitrogen), as appropriate, with reactions for 1 h at room temperature on a shaker. Cells were visualized using an Operetta confocal plate reader (PerkinElmer). Flow cytometry was also used to assess surface markers associated with pluripotency. Cells were fixed in 4% paraformaldehyde in suspension for 15 min at room temperature. Cells were then centrifuged for 5 min at 160 *g*. The pellet was then washed in phosphate-buffered saline once before being centrifuged at 160 *g* again. The cell pellet was then resuspended and stained for TRA-1-81 (mouse, 1:100, 12-8883-82; eBioscience), SSEA4 (mouse, 1:100, 12-8843-42; eBioscience), and SSEA1 (mouse, 1:100, 12-8813-42; eBioscience). Flow cytometry was performed on MoFlo (Beckman Coulter).

Differentiation of hiPSC-CMs

Human iPSCs were seeded at $9 \times 10^4/cm^2$ and allowed to reach >90% confluence (approximately by d3) with daily changes in E8 medium. The medium was then changed to StemPro34 supplemented with 1 ng/mL BMP4. Next day, the medium was changed to fresh StemPro34 supplemented with 5 ng/mL BMP4 and 8 ng/mL Activin A for 48 h. The medium was then changed to RPMI B27 (minus insulin) supplemented with 10 nM KY02111 and XAV939, and then incubated for 48 h. The medium was then changed to RPMI B27 supplemented with 10 nM KY02111 and XAV939 and incubated for 48 h. After this time, cells were cultured routinely in RPMI B27 with medium changes every 2–3 days.

Assessment of electrophysiology

The CellOPTIQ platform [15] was used to record optical-based action potentials from hiPSC-CMs. Cells were seeded into Matrigel-coated 96-well plates at a density of 50,000 cells per well. These hiPSC-CMs were then incubated at 37°C and 5% CO_2 for 48 h to allow cells to recover. To image the voltage properties of the hiPSC-CMs, they were dyed using FluoVolt (F10488). Media were removed from wells and serum-free media (SFM) (DMEM +0.5 M galactose (Sigma-Aldrich) and 100 mM sodium pyruvate) containing FluoVolt (PartA: 0.5 μL/mL and PartB: 5 μL/mL) were added; these cells were incubated at 37°C and 5% CO_2 for 30 min. After the 30-min incubation, the medium was removed and the hiPSC-CMs washed once with SFM before 100 μL of fresh SFM was added to wells. These plates were then incubated at 37°C and 5% CO_2 for 15 min to allow the hiPSC-CMs to equilibrate before recording traces.

For drug treatment, a basal recording was taken before 20 μL of drug was added to the well; all drugs were dissolved in dimethyl sulfoxide (DMSO) and added to the cells with a 0.1% DMSO concentration. After this addition, the hiPSC-CMs were incubated at 37°C and 5% CO_2 for 30 min before a second measurement was taken. The drugs used in the study were all purchased from Sigma: Telmisartan (Cat: T8949); GW0742, (Cat: G3295); NS1643 (Cat: N0663); Ginsenoside RG3 (Cat: SML0184); Minoxidil (Cat: M4145); and Nicorandil (Cat N3539).

Voltage data were analyzed using CellOPTIQ proprietary software of Clyde Biosciences and were normalized to a maximum amplitude of 1 and minimum of 0 to standardize height for comparison of traces created in Origin software package.

Results

Derivation and characterization of LQTS2-hiPSC-CMs

Skin fibroblasts were derived under informed consent from a 19-year-old LQTS2 patient when she received a preventative implantable cardioverter defibrillator, as previously described [10]. Clinically, the patient had experienced polymorphic ventricular tachyarrhythmia at rates of 230 bpm and had a QTc of up to 571 ms on the electrocardiogram (Fig. 1A). Genotyping showed an LQTS2-associated autosomal dominant point mutation c.*G1681A* (p.A561T) in *KCNH2*.

Following integration-free reprogramming of the skin fibroblasts with recombinant *OCT4*, *SOX2*, *cMYC*, and *KLF4* Sendai viruses, single colonies of LQTS2-hiPSCs were picked and expanded in E8 culture medium on Matrigel. Immunostaining and image analysis showed that nearly all cells expressed the transcription factors, OCT4, SOX2, and NANOG (Fig. 1B). This was cross-confirmed by positive staining by flow cytometry to the surface markers, TRA1-81 and SSEA4, but not the differentiation marker, SSEA1 (Fig. 1C). Cultures were routinely passaged at a ratio of 1:8 ($\sim$20,000 cells/cm^2) and harvested 3 days later, equating to a population doubling rate of $\sim$24–27 h, which is consistent with the wider literature [16]. Karyotyping of 30 metaphase spreads and assembly of homologous chromosomes into a karyogram showed no abnormalities (Fig. 1D). Genotyping of the LQTS2-hiPSC line confirmed the c.*G1681A* mutation (Fig. 1E). Directed monolayer differentiation protocol produced beating sheets of CMs that were >80% positive for α-actinin staining (Fig. 1F).

To examine electrophysiology characteristics, confluent monolayers of LQTS-hiPSC-CMs were established in 96-well plates and loaded with the voltage-sensitive dye, FluoVolt. Optical traces were recorded and analyzed using the CellOPTIQ platform, as previously described [17]. For comparison, hiPSC-CMs were also produced from skin fibroblasts donated by the LQTS2 patient's father, who was considered healthy with no *G1681A* mutation, no electrical anomalies in heart function (electrocardiogram QTc of 455 ms), and no clinical symptoms. Averaged traces (Fig. 1G) confirmed significantly prolonged APDs in LQTS2-hiPSC-CMs relative to hiPSC-CMs from the healthy father, with respective values for APD_{50} of 374 ± 25 ms versus 348 ± 47 ms, APD_{90} of 443 ± 31 ms versus 404 ± 42 ms, and triangularization ($APD_{90} - APD_{30}$) of 158 ± 15 ms versus 120 ± 12 ms (Fig. 1G; all $P < 0.05$ by unpaired *t*-test).

Since the LQTS2 patient's treatment includes β-blockers, such as the nonspecific β1- and β2-adrenoceptor antagonist, propranolol, we wished to evaluate the effect of this drug on action potential characteristics of the corresponding LQTS-hiPSC-CMs. Using the same voltage-sensitive dye as above, baseline action potentials were recorded for 30 min before adding propranolol at 5×½ log concentration increases from 10 to 1,000 nM, an approach also adopted for all subsequent drug tests. For propranolol, calculation of percentage change in APD_{50}, APD_{90}, and triangularization showed marginal change only, occasionally bordering on significance (Fig. 1H).

Effect of I_{Kr} modulators on the action potential of LQTS2-hiPSC-CMs

We have previously shown that the *G1681A* mutation in *KCNH2* disrupts trafficking of the I_{Kr}/HERG channel to the cell membrane [18]. The channel comprises a tetrameric complex and the mutation is autosomal dominant negative. This means that even when the healthy and mutant *KCNH2* alleles are expressed at equal 1:1 ratios, only 6% of I_{Kr} channels are functional because one or more mutant proteins in the tetrameric complex compromises channel function [18]. This explains why LQTS2 is associated with such dramatic increases in QT interval. Therefore, we wished to evaluate whether different drugs could reduce the APD in LQTS-hiPSC-CMs.

Because I_{Kr} is still at least partially active in LQTS2-hiPSC-CMs with the *G1681A* mutation, we first evaluated whether chemicals that interact directly with this channel could shorten APD. Ginsenoside RG3 is known to modulate I_{Kr} by interacting with a Ser631 residue the channel pore entryway, which decelerates channel deactivation [19]. A second compound, NS1643, changes the voltage dependence of inactivation, which has previously led to an increase in steady state and tail currents in *Xenopus laevis* oocytes engineered to overexpress the HERG channel [20]. As before, a ½ log range from 10 to 1,000 nM was used in combination with the CellOPTIQ to measure optical recordings from LQTS2-hiPSC-CMs loaded with FluoVolt (Fig. 2). The effect of Ginsenoside RG3 was relatively modest on APD, with significant reductions reached at ≥100 nM and only then equating to around an 8% reduction in APD90 and triangularization (Fig. 2A, Bi). In contrast, at multiple concentrations, NS1643 caused highly significant reductions in all three parameters, APD_{50}, APD_{90}, and triangularization, with the maximum concentration leading to a reduction of nearly 20%. A change in the action potential morphology was also seen, as indicated by significant reduction in triangularization (Fig. 2A, Bii).

We wished to determine whether alternative methods of enhancing I_{Kr} may be beneficial to the action potential characteristics of LQTS-hiPSC-CMs. It has been reported that the PPARδ pathway targets protein 14-3-3 epsilon, which in turn interacts with HERG to stabilize the PKA-phosphorylated state of the channel by shielding phosphates from degradation [21]. Therefore, we selected two PPARδ agonists, Telmisartan and GW0742 [22,23], using them across the same concentration ranges described above (Fig. 3). Overall, the observed effect on APD_{50}, APD_{90}, and triangularization of LQTS2-hiPSC-CMs treated with Telmisartan and GW0742 was similar to that seen for NS1643. Thus, reduction in APD_{50} and APD_{90} was highly significant at many of the concentrations used (Fig. 3). The impact of GW0742 was particularly dramatic, with the maximum concentration tested causing a reduction of $\sim$20% for both APD_{50} and APD_{90}, and $\sim$14% for triangularization (Fig. 3).

Effect of I_{KATP} modulators on the action potential of LQTS2-hiPSC-CMs

Finally, we sought to evaluate whether modulation of other potassium currents, including I_{KATP}, would be beneficial to the action potential characteristics of LQTS CMs. Nicorandil has dual properties in that it activates potassium channels to enhance efflux and has hyperpolarizing effects by inhibiting voltage-gated calcium channels [24]. The sulfated form of Minoxidil causes relaxation of vascular smooth muscle by opening IK_{ATP} channels [25]. Overall, the

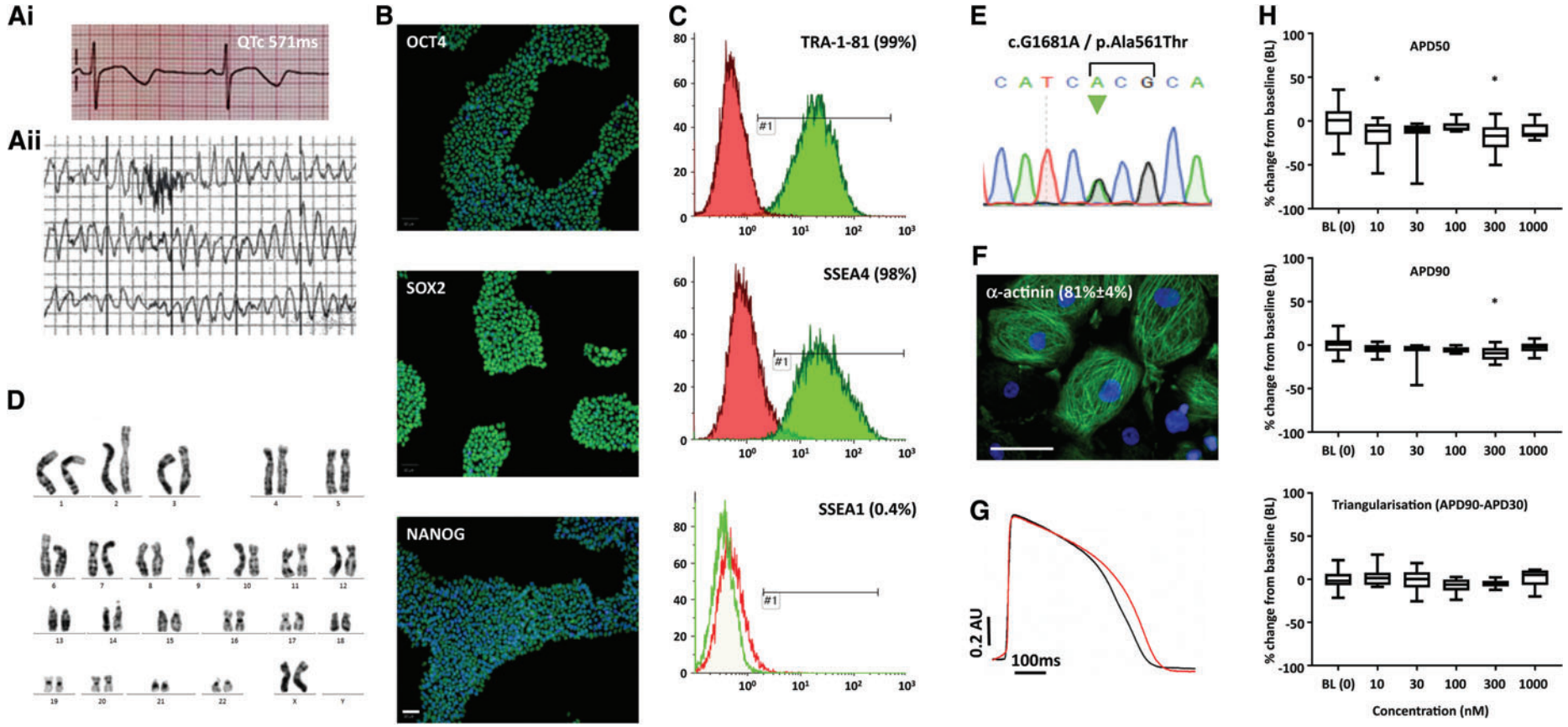

FIG. 1. Generation and characterization of a LQTS2-hiPSC line. **(A)** Shows the electrocardiogram of the LQTS2 patient during rest, with QTc of up to 571 ms **(Ai)**, and during an arrhythmic episode **(Aii)**. After harvesting skin samples from the patient and using Sendai-based reprogramming, the resulting hiPSC line was shown to express markers of pluripotency by immunostaining **(B)** and flow cytometry **(C)**. The LQTS2 hiPSCs showed a normal karyotype **(D)** and was heterozygote for the G/A mutation at nucleotide position 1,681 in the *KCNH2* gene **(E)**. Directed monolayer differentiation produced hiPSC-CMs of >80% purity **(F)**. Optical recordings using the voltage-sensitive dye, FluoVolt, were made on the CellOPTIQ platform and showed that the APD of LQTS2-hiPSC-CMs (*red* trace) was prolonged relative to hiPSC-CMs derived from her healthy father (*black* trace; **G**). In **(H)**, LQTS2-hiPSC-CMs were assessed at baseline and after treatment with a 10–1,000 nM concentration range of the nonspecific β-blocker, propranolol, which shows marginal impact on APD. Data are mean ± SEM with 40 replicates for BL (0) and 8 replicates for all other treatments; Dunnett's test; $*P \leq 0.05$. Scale bars = 100 μm. APD, action potential duration; CMs, cardiomyocytes; hiPSC, human induced pluripotent stem cell; LQTS, long QT syndrome; QTc, corrected QT; SEM, standard error of the mean. Color images available online at www.liebertpub.com/scd

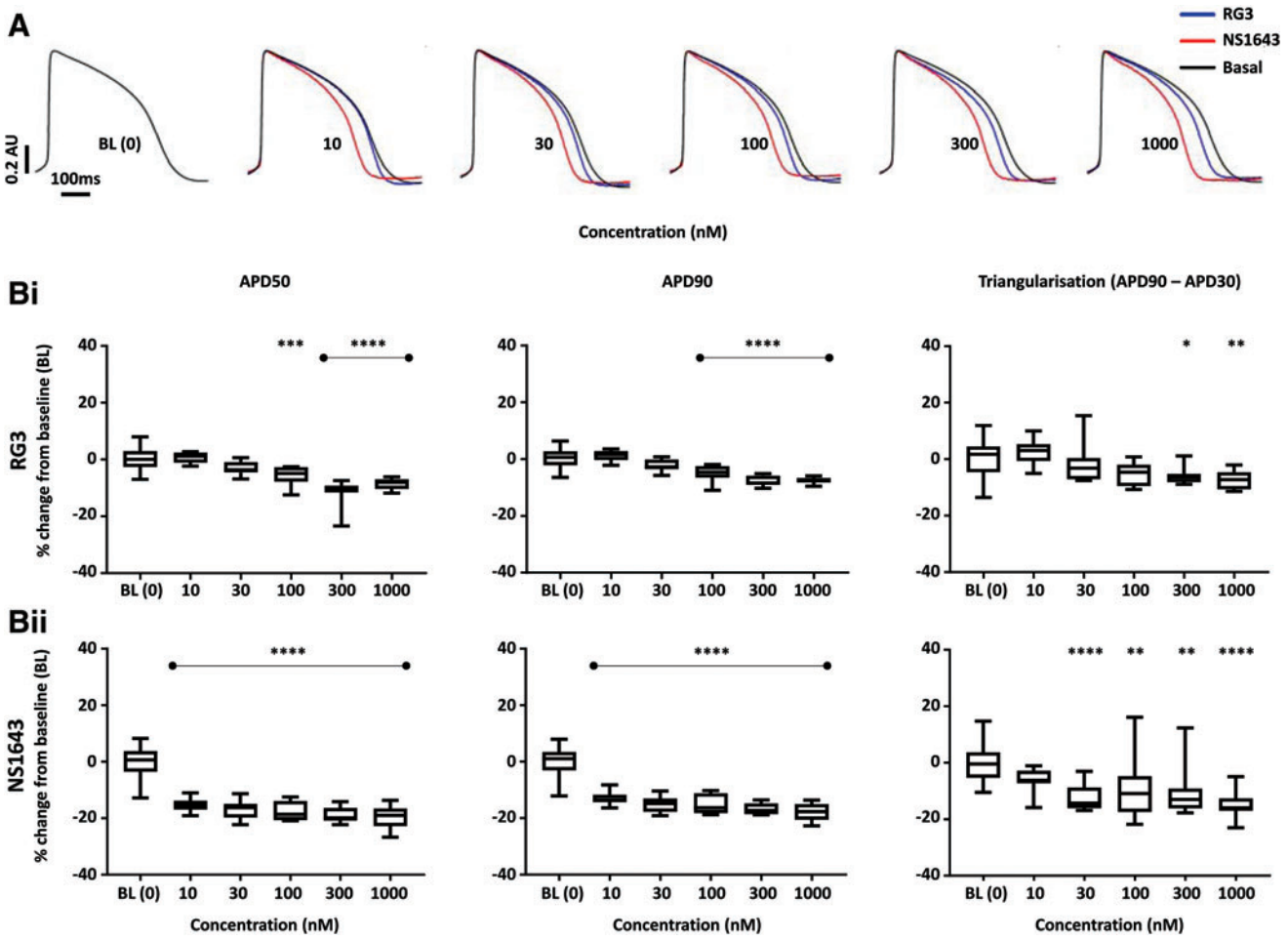

FIG. 2. Direct modulation of I_{Kr} channels. LQTS2-hiPSC-CMs were treated with the plant constituent, Ginsenoside RG3, or the synthetic compound, NS1643. After loading with the voltage-sensitive dye, FluoVolt, optical recordings were made using the CellOPTIQ platform. Averaged traces across the concentration range are shown in **(A)**, while the derived percentage changes in APD_{50}, APD_{90}, and triangularization are shown in **(Bi**; RG3**)** and **(Bii**; NS1643**)**. Data are mean ± SEM with 40 replicates for BL (0) and 8 replicates for all other treatments; Dunnett's test comparison to baseline (BL [0]); $*P \leq 0.05$; $**P \leq 0.01$; $***P \leq 0.001$; $****P \leq 0.0001$. Color images available online at www.liebertpub.com/scd

observed effect on APD_{50} and APD_{90} of LQTS2-hiPSC-CMs of Minoxidil and Nicorandil was similar to that seen for NS1643, Telmisartan, and GW0742. Highly significant reduction in these parameters was seen through the concentration ranges, with the highest concentration causing a reduction of up to 19% (Fig. 4). While the impact on triangularization was less pronounced, significant reductions were seen for Minoxidil, particularly at higher concentrations (Fig. 4).

Discussion

We seized the opportunity to harvest skin cells from an LQTS2 patient undergoing surgery to receive preventative implantable cardioverter defibrillator. Integration-free hiPSCs were produced and the derived CMs were used to evaluate impact of drugs on APD as an in vitro surrogate measurement of QT interval. While the β-blocker, propranolol, failed to meaningfully reduce APD in LQTS-hiPSC-CMs, direct or indirect interaction of compounds with I_{Kr} and I_{KATP} channel was able to induce reductions of up to 21%. The use of indirect activation of I_{Kr} by modulation of the PPARδ pathway was of particular importance as it highlights a new potential route for therapeutic intervention of LQTS2, which should be explored further in the future.

A feature often highlighted with regard to recombinant Sendai virus reprogramming is that it is integration free and viral-derived transcripts are readily diluted within the first few passages after hiPSC lines are established. Contrary to this notion, our routine checks for persistence of transgene expression by reverse transcription polymerase chain reaction at passages ~15 after hiPSC derivation were positive for cMYC. Indeed, when we surveyed eight of the hiPSC lines in our laboratory produced using the CytoTune2.0 recombinant Sendai virus system, expression analysis showed 50% and 12.5% were positive for cMYC and KLF4, respectively, although none was positive for polycistronic KLF4–OCT3/4–SOX2. Nevertheless, residual transgene expression did not impact pluripotency marker expression, stable karyotype, or high efficiency-directed monolayer differentiation into functional CMs, with values

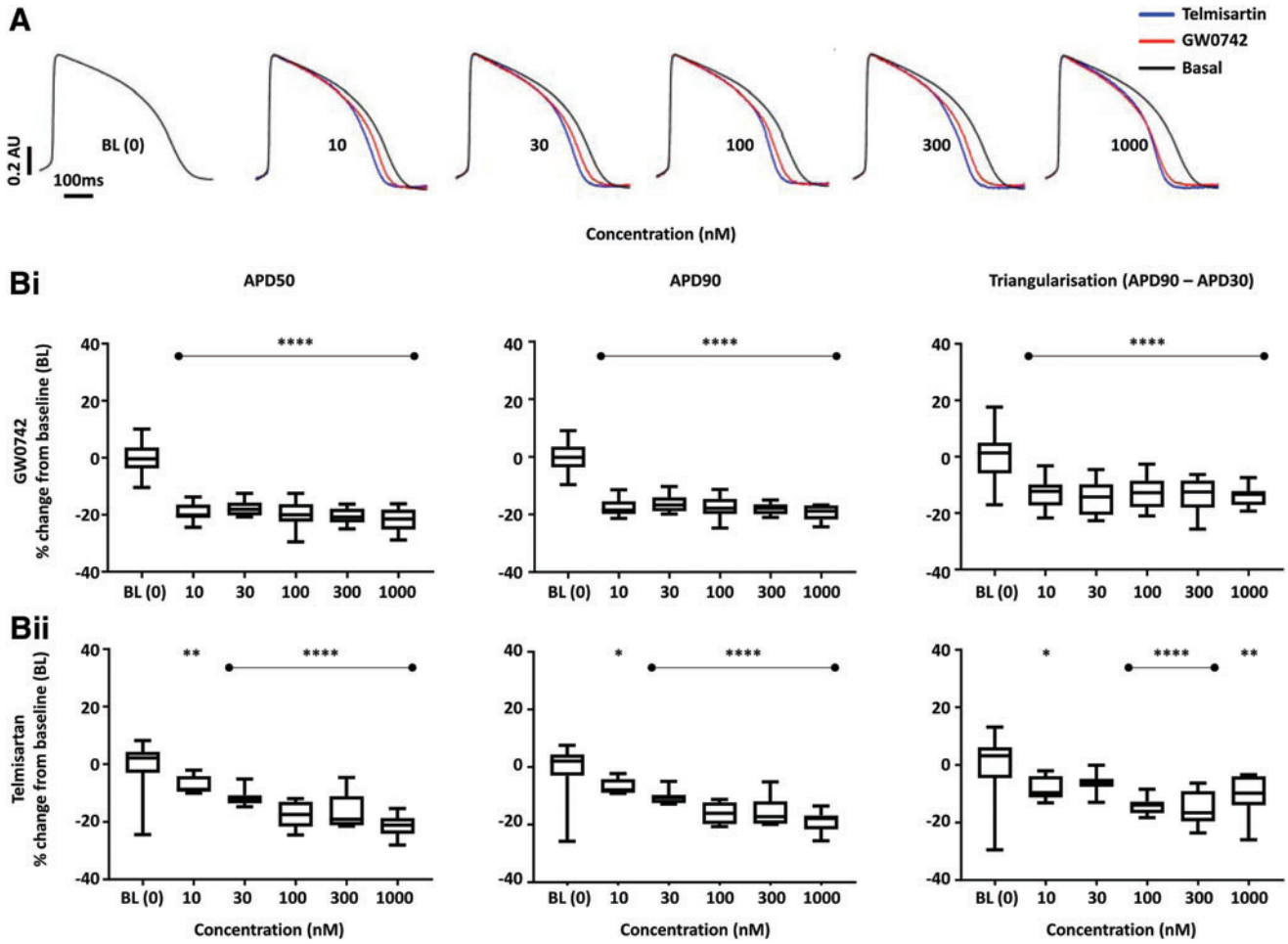

FIG. 3. Indirect modulation of I_{Kr} channels with PPARδ agonists. LQTS2-hiPSC-CMs were treated with the PPARδ agonists, GW0742, and Telmisartan, which are thought to stabilize the PKA-phosphorylated state of HERG by protein 14-3-3 epsilon. After loading with the voltage-sensitive dye, FluoVolt, optical recordings were made using the CellOPTIQ platform. Averaged traces across the concentration range are shown in **(A)**, while the derived percentage changes in APD_{50}, APD_{90}, and triangularization are shown in **(Bi**; GW0742**)** and **(Bii**; Telmisartan**)**. Data are mean ± SEM with 40 replicates for BL (0) and 8 replicates for all other treatments; Dunnett's test comparison to baseline (BL [0]); $*P \leq 0.05$; $**P \leq 0.01$; $***P \leq 0.001$; $****P \leq 0.0001$. Color images available online at www.liebertpub.com/scd

for each matching best in class published elsewhere in the literature [26,27]. This provided an opportunity to use the LQTS-hiPSC-CMs to evaluate the impact of drugs on APD, which is an in vitro surrogate for QT interval on the electrocardiogram.

Although β-blocker therapy is highly efficacious and successful for most LQTS1 patients, it is often insufficient as a standalone treatment for LQTS2, where up to 23% of patients continue to experience cardiac events [7]. This notion was supported by our data with propranolol, which showed a marginal effect on APD in LQTS-hiPSC-CMs. This result was expected because propranolol is a nonspecific β1- and β2-adrenoceptor inhibitor that works by competitive binding to outcompete chronotropic agents, such as isoprenaline [28,29]. However, the underlying cause of altered CM function in LQTS2 is not beat rate, but rather excessively long QT interval, which is not treated with β-blockers.

It is not surprising that nearly half of the genotyped cases for LQTS are due to mutations in *KCNH2*. The I_{Kr}/HERG channel is the major driving force behind phase 3 repolarization during the cardiac action potential [30]. Furthermore, the I_{Kr} channel is formed from a tetrameric complex, and its ability to be trafficked to the cell membrane and/or flux potassium ions is compromised if one or more of the four proteins is mutated [31]. It is for this reason that even when expression ratios of healthy and mutant alleles of KCNH2 are equal at 50% each, only 6% of ion channels are predicted to be functional [18]. This makes it all the more important to find methods that amplify the activity of the remaining functional channels.

For each of the drugs we used to modulate ion channel function, a 5×½ log concentration range was used. While some drugs have previously been used on CMs in culture (eg, Nicorandil [10] and NS1643 [32]), several others had not been, and we relied on ranges that spanned published concentrations, including those used in cancer cell lines, neuronal cultures, and human mesangial cells [33–35]. Nicorandil has previously been shown to be effective in reducing APD by 19% in integrating lentivirally derived LQTS-hiPSC-CMs, as measured from action potentials

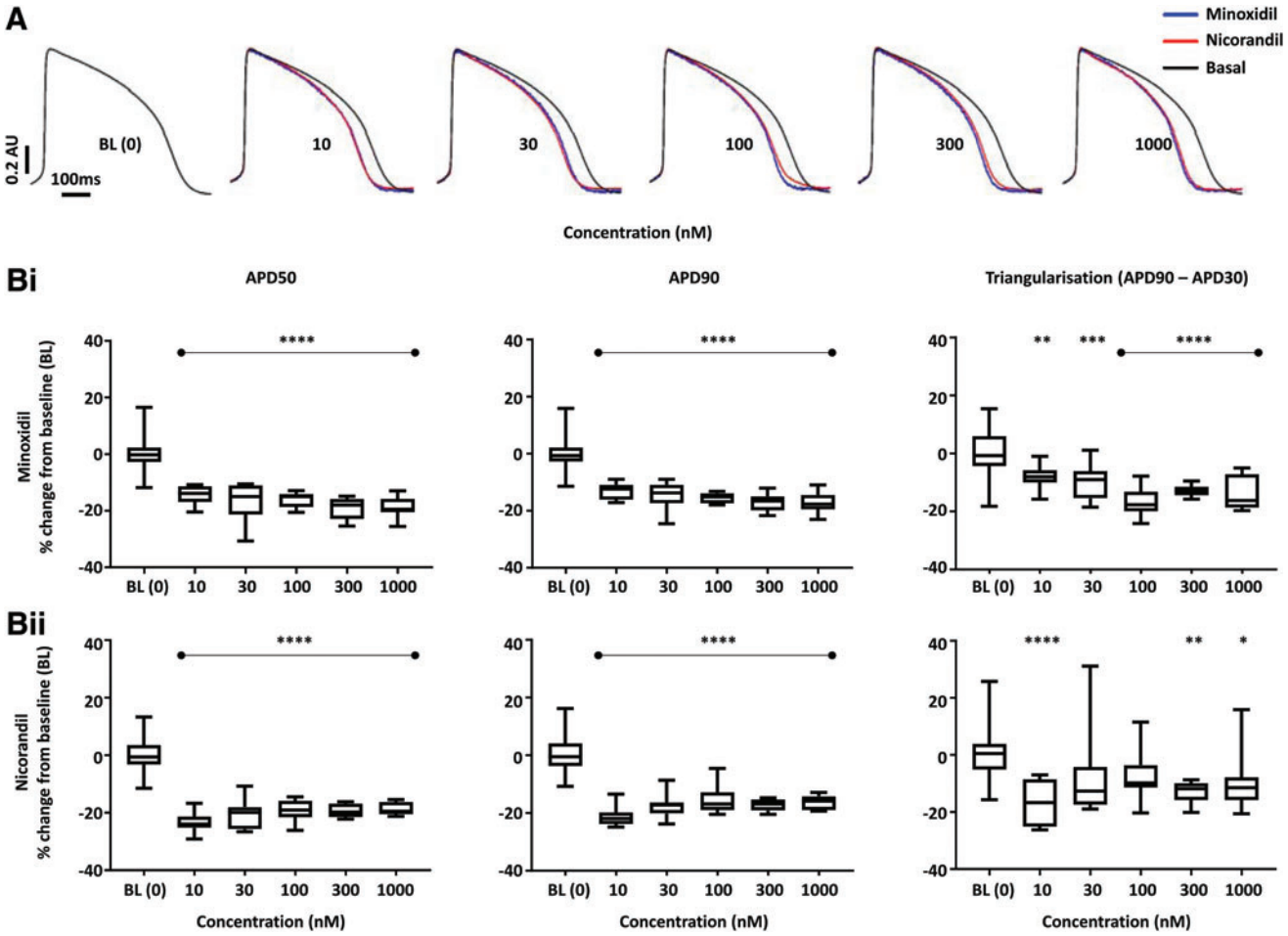

FIG. 4. Modulation of I_{KATP}. LQTS2-hiPSC-CMs were treated with the I_{KATP} enhancers, Minoxidil and Nicorandil. After loading with the voltage-sensitive dye, FluoVolt, optical recordings made using the CellOPTIQ platform. Averaged traces across the concentration range are shown in **(A)**, while the derived percentage changes in APD_{50}, APD_{90}, and triangularization are shown in (**Bi**; Minoxidil) and (**Bii**; Nicorandil). Data are mean ± SEM with 40 replicates for BL (0) and 8 replicates for all other treatments; Dunnett's test comparison to baseline (BL [0]); $*P \leq 0.05$; $**P \leq 0.01$; $***P \leq 0.001$; $****P \leq 0.0001$. Color images available online at www.liebertpub.com/scd

using conventional single-cell patch clamp or extracellular field potentials using multicellular aggregates on multi-electrode arrays [10]. That study used a single, unspecified concentration of Nicorandil; so it is difficult to know exactly how this relates to our data for this I_{KATP} opener. We observed a reduction in APD_{90} ranging from −15% to −22% with the concentrations tested. Clinical dosage of Nicorandil is as 40 mg tablets that lead to a plasma C_{max} of 300 ng/mL (1,420 nM) 30 min postadministration [36]. This is greater than our highest concentration, consistent with the clinical use of Nicorandil in treatment of ventricular tachycardia [37], and so opens the possibility for evaluation in LQTS2 patients.

We also tested Minoxidil as an alternative modulator of I_{KATP}, where APD_{90} reduction associated well with concentration to a maximum of −17% at 1,000 nM. Minoxidil is most commonly used as a topical treatment in hair products for alopecia [38]. For internal use, the maximum permitted dose is 100 mg, but more commonly, the range is up to 40 mg daily, where it acts as a powerful peripheral vasodilator for treatment of hypertension [39], and is often used with β-blockers [40]. This would make for a useful combination in LQTS, where β-blockers control increase in heart rate from the sympathetic nervous system stimulation, while Minoxidil reduces the QT interval. Nevertheless, Minoxidil would need to be used with some level of caution. In humans, one side effect is hypertrichosis (excessive hair growth) by increasing expression of dermal papilla markers [41], hence its common use in hair growth products [42]. Also, studies in dogs have shown that cardiovascular toxicity occurs at ∼17 ng/mL [43], which equates to 80 nM. Therefore, it is promising that even at the lowest concentration we tested (10 nM), highly significant reductions of ∼14% were seen for APD_{50} and APD_{90} in LQTS-hiPSC-CMs.

Although the number of active I_{Kr} channels in LQTS2 patients is low, this current still remains a realistic target. Previously, it was shown [18] that reducing expression of the mutant *KCNH2* transcript by allele-specific RNA interference in LQTS-hiPSC-CMs boosted the number of active channels from 6% to 27%. This abolished arrhythmias and reduced QT interval. However, while this approach worked

well in vitro using siRNA or lentivirally delivered shRNAs, the density and quantity of myocardium in the human heart make this a challenging proposition in patients [44]. It is possible that AAV or peptide delivery vehicles [45,46] may overcome this issue.

In the immediate future, chemical modulation of I_{Kr}/HERG is a more feasible route. Most drug interaction with this channel induces prolongation of QT interval and is a major risk factor that is considered in pharmaceutical drug development [47]. Indeed, as part of an international initiative, termed CiPA (Comprehensive in Vitro Proarrhythmia Assay), healthy hiPSC-CMs are being evaluated for their effectiveness as an early detection system for drug-induced arrhythmias, including HERG blockers [48]. We have previously shown [18] that in both healthy and LQTS2 hiPSC-CMs (*KCNH2 G1681A*), specific chemical blockade of HERG with E4031 caused prolongation of field potential duration and APD by up to 52% and 77%, respectively. Arrhythmic-like events were detected in ~30% of cases, but only in the LQTS2-hiPSC-CMs. This confirms two key points regarding LQTS2 CMs: (1) they show increased susceptibility to drug-induced APD prolongation and arrhythmias; and (2) the residual I_{Kr} current is still sufficient to be a pharmacological target, prolonging in this case, but prompting us to evaluate four compounds for their ability to shorten QT interval.

Within this background context, direct chemical interaction with HERG was investigated using Ginsenoside RG3 and NS1643. Derived as a pharmacologically active natural constituent of plants of the genus *Panax* [49], RG3 exhibits an antiapoptotic and anti-inflammatory effect shown to improve cardiac function in rat models of myocardial infarction [50]. RG3 also interacts with I_{Kr}, at the channel pore entryway to decelerate deactivation, and I_{Ks}, through the KCNE1 subunit that co-assembles with KCNQ1 [51,52]. Only higher concentrations of RG3 were effective in reducing APD_{50} and APD_{90} in LQTS-hiPSC-CMs, and there was no effect on triangularization. This may be because binding of RG3 to the serine residue in the pore of I_{Kr} is weak. Also, the impact of RG3 on I_{Ks} activation is likely to be minimal because this current is relatively small and there has been controversy over whether it makes a meaningful contribution to repolarization in hiPSC-CMs [53,54]. For NS1643, we observed potent responses at all concentrations tested, which was surprising. While others have shown acceleration of repolarization in hiPSC-CMs, the concentrations used have been substantially higher at up to 30 μM [55] or >100 μM [56] than those we used (10–1,000 nM). The reasons for these differences are unclear, but may include mutation type (LQTS2 p.N996I vs. p.A561T) or the method used to assess electrophysiology, wherein these articles used multielectrode arrays to record extracellular field potentials, while we used optical recording of changes in the voltage-sensitive dye, FluoVolt. This also potentially highlights the challenge of cross-comparing data from different platforms or cellular configurations. Indeed, simply plating hiPSC-CMs at different densities appears to change APD morphology and cardiac chamber specificity [57]. Therefore, while it would be interesting to test the influence of these drugs on the activity of specific ion channels, this would necessitate switching from hiPSC-CMs in a continuous monolayer using optical dyes on the CellOPTIQ to isolated single cells using manual patch clamp, which could confound data interpretation. Moreover, the high level of heterogeneity associated with single CMs derived from hiPSC-CM populations [58] means large numbers cells need to be patched to reach statistical confidence.

Perhaps most interestingly, we were also able to use an indirect approach to enhance I_{Kr} activity and hence reduce QT interval. The PPARδ pathway is pleotropic and associated with regulation of many processes, ranging from metabolism, diabetes, and hypertension to cancer [35,59–62]. However, some literature, including in endothelial cell biology, suggests PPARδ pathway agonists stimulate expression of *YWHAE* [63], whose gene product, 14-3-3 epsilon, activates the HERG channel [21]. Therefore, we selected two drugs that targeted the PPARδ pathway. Telmisartan was approved for use by the FDA in 2014 with potential uses in fibrosis, type 2 diabetes, and hypertension. The second compound was GW0742, which has a high specificity (EC_{50} of 1 nM) to PPARδ. GW0742 has been used experimentally to reduce lung inflammation in mice [64] and has been shown to have cardioprotective effect against ischemic injury in rats [65]. Since PPARδ agonists have not previously been evaluated for their ability to reduce QT interval in LQTS, it was notable that at all concentrations tested for GW0742 and nearly all for Telmisartan, significant reductions in APD_{50}, APD_{90}, and triangularization were observed. This suggests that PPARδ agonists could form a new class of drugs to treat LQTS2.

Nevertheless, further investigation will be required for these PPARδ agonists. They may also function through other pathways and their dosage will be important. For Telmisartan, we found highly significant benefit to APD characteristics in LQTS2 hiPSC-CMs starting at 30 nM. However, studies using doses of 1,000-fold higher (30 and 100 μM) in vivo in rats led to Na^+ and Ca^{++} overload, cardiac dysfunction, and CM death [66]. Also, Telmisartan has an angiotensin receptor blocking activity and can modulate PPARγ [67]; so we cannot rule out activity through these pathways. The same is true for GW0742, which binds to PPARα or PPARγ, although with an affinity of at least 300-fold lower than to PPARδ [68]. All three PPAR isoforms are expressed in the heart [69]. Thus, it is notable that both PPARδ and PPARγ have been shown to associate with 14-3-3 epsilon [70], creating connectivity to the HERG channel. Given the higher specificity of GW0742 to PPARδ and the additional PPARγ:14-3-3 epsilon:HERG pathway, this may be the drug of choice for further studies in LQTS.

In conclusion, we showed that six different direct or indirect channel modulators could reduce the APD characteristics of LQTS2-hiPSC-CMs. The rank order (highest to lowest) of these agents for change in APD_{90} at the minimum concentration (10 nM) was Nicorandil (−21%) > GW0742 (−18%) > NS1643 (−13%) = Minoxidil (−13%) > Telmisartan (−7%) > RG3 (+1%), while at the maximum concentration (1,000 nM), it was NS1643 (−20%) > GW0742 (−19%) = Telmisartan (−19%) > Minoxidil (−17%) > Nicorandil (−16%) > RG3 (−7%). This should be useful information when evaluating ion channel modulators in the context of LQTS; the next steps will be to examine the effect of these drugs in CMs from a wider range of hiPSC lines carrying the same or different *KCNH2* mutations.

Acknowledgments

This work was supported by the British Heart Foundation [SP/15/9/31605., RG/15/6/31436., PG/14/59/31000., RG/14/1/30588., P47352/Centre for Regenerative Medicine]; BIRAX [04BX14CDLG]; Medical Research Council [MR/M017354/1]; The National Centre for the Replacement, Refinement and Reduction of Animals in Research (NC3Rs) [CRACK-IT. FULL PROPOSAL code 35911-259146., NC/K000225/1]; and Heart Research UK [TRP01/12]. Funding for open access charge: British Heart Foundation.

Author Disclosure Statement

No competing financial interests exist. G.S.: Chief Scientific Officer and Co-Founder of Clyde Biosciences.

References

1. Giudicessi JR and MJ Ackerman. (2013). Genotype- and phenotype-guided management of congenital long QT syndrome. Curr Probl Cardiol 38:417–455.
2. Crotti L, G Celano, F Dagradi and PJ Schwartz. (2008). Congenital long QT syndrome. Orphanet J Rare Dis 3:18.
3. Medeiros-Domingo A, P Iturralde-Torres and MJ Ackerman. (2007). [Clinical and genetic characteristics of long QT syndrome]. Rev Esp Cardiol 60:739–752.
4. Schwartz PJ, L Crotti and R Insolia. (2012). Long-QT syndrome: from genetics to management. Circ Arrhythm Electrophysiol 5:868–877.
5. Ioakeimidis NS, T Papamitsou, S Meditskou and Z Iakovidou-Kritsi. (2017). Sudden infant death syndrome due to long QT syndrome: a brief review of the genetic substrate and prevalence. J Biol Res (Thessalon) 24:6.
6. Abu-Zeitone A, DR Peterson, B Polonsky, S McNitt and AJ Moss. (2014). Efficacy of different beta-blockers in the treatment of long QT syndrome. J Am Coll Cardiol 64:1352–1358.
7. Priori SG, C Napolitano, PJ Schwartz, M Grillo, R Bloise, E Ronchetti, C Moncalvo, C Tulipani, A Veia, G Bottelli and J Nastoli. (2004). Association of long QT syndrome loci and cardiac events among patients treated with beta-blockers. JAMA 292:1341–1344.
8. Vincent GM, PJ Schwartz, I Denjoy, H Swan, C Bithell, C Spazzolini, L Crotti, K Piippo, JM Lupoglazoff, et al. (2009). High efficacy of beta-blockers in long-QT syndrome type 1: contribution of noncompliance and QT-prolonging drugs to the occurrence of beta-blocker treatment ''failures.'' Circulation 119:215–221.
9. Moretti A, M Bellin, A Welling, CB Jung, JT Lam, L Bott-Flügel, T Dorn, A Goedel, C Höhnke, et al. (2010). Patient-specific induced pluripotent stem-cell models for long-QT syndrome. N Engl J Med 363:1397–1409.
10. Matsa E, D Rajamohan, E Dick, L Young, I Mellor, A Staniforth and C Denning. (2011). Drug evaluation in cardiomyocytes derived from human induced pluripotent stem cells carrying a long QT syndrome type 2 mutation. Eur Heart J 32:952–962.
11. Ma D, H Wei, Y Zhao, J Lu, G Li, NB Sahib, TH Tan, KY Wong, W Shim, et al. (2013). Modeling type 3 long QT syndrome with cardiomyocytes derived from patient-specific induced pluripotent stem cells. Int J Cardiol 168: 5277–5286.
12. Yazawa M, B Hsueh, X Jia, AM Pasca, JA Bernstein, J Hallmayer and RE Dolmetsch. (2011). Using induced pluripotent stem cells to investigate cardiac phenotypes in Timothy syndrome. Nature 471:230–234.
13. Davis RP, S Casini, CW van den Berg, M Hoekstra, CA Remme, C Dambrot, D Salvatori, DW Oostwaard, AA Wilde, et al. (2012). Cardiomyocytes derived from pluripotent stem cells recapitulate electrophysiological characteristics of an overlap syndrome of cardiac sodium channel disease. Circulation 125:3079–3091.
14. Itzhaki I, L Maizels, I Huber, A Gepstein, G Arbel, O Caspi, L Miller, B Belhassen, E Nof, M Glikson and L Gepstein. (2012). Modeling of catecholaminergic polymorphic ventricular tachycardia with patient-specific human-induced pluripotent stem cells. J Am Coll Cardiol 60:990–1000.
15. Hortigon-Vinagre MP, V Zamora, FL Burton, J Green, GA Gintant and GL Smith. (2016). The use of ratiometric fluorescence measurements of the voltage sensitive dye di-4-ANEPPS to examine action potential characteristics and drug effects on human induced pluripotent stem cell-derived cardiomyocytes. Toxicol Sci 154:320–331.
16. Nakagawa M, Y Taniguchi, S Senda, N Takizawa, T Ichisaka, K Asano, A Morizane, D Doi, J Takahashi, et al. (2014). A novel efficient feeder-free culture system for the derivation of human induced pluripotent stem cells. Sci Rep 4:3594.
17. Blinova K, J Stohlman, J Vicente, D Chan, L Johannesen, MP Hortigon-Vinagre, V Zamora, G Smith, WJ Crumb, et al. (2017). Comprehensive translational assessment of human-induced pluripotent stem cell derived cardiomyocytes for evaluating drug-induced arrhythmias. Toxicol Sci 155:234–247.
18. Matsa E, JE Dixon, C Medway, O Georgiou, MJ Patel, K Morgan, PJ Kemp, A Staniforth, I Mellor and C Denning. (2014). Allele-specific RNA interference rescues the long-QT syndrome phenotype in human-induced pluripotency stem cell cardiomyocytes. Eur Heart J 35:1078–1087.
19. Choi SH, TJ Shin, SH Hwang, BH Lee, J Kang, HJ Kim, SH Jo, H Choe and SY Nah. (2011). Ginsenoside Rg(3) decelerates hERG K(+) channel deactivation through Ser631 residue interaction. Eur J Pharmacol 663:59–67.
20. Casis O, SP Olesen and MC Sanguinetti. (2006). Mechanism of action of a novel human ether-a-go-go-related gene channel activator. Mol Pharmacol 69:658–665.
21. Kagan A, YF Melman, A Krumerman and TV McDonald. (2002). 14-3-3 amplifies and prolongs adrenergic stimulation of HERG K+ channel activity. EMBO J 21:1889–1898.
22. Feng X, Z Luo, L Ma, S Ma, D Yang, Z Zhao, Z Yan, H He, T Cao, D Liu and Z Zhu. (2011). Angiotensin II receptor blocker telmisartan enhances running endurance of skeletal muscle through activation of the PPAR-δ/AMPK pathway. J Cell Mol Med 15:1572–1581.
23. Luquet S, C Gaudel, D Holst, J Lopez-Soriano, C Jehl-Pietri, A Fredenrich and PA Grimaldi. (2005). Roles of PPAR delta in lipid absorption and metabolism: a new target for the treatment of type 2 diabetes. Biochim Biophys Acta 1740:313–317.
24. Kukovetz WR, S Holzmann and G Pöch. (1992). Molecular mechanism of action of nicorandil. J Cardiovasc Pharmacol 20 (Suppl 3):S1–S7.
25. Messenger AG and J Rundegren. (2004). Minoxidil: mechanisms of action on hair growth. Br J Dermatol 150: 186–194.
26. Akopian V, PW Andrews, S Beil, N Benvenisty, J Brehm, M Christie, A Ford, V Fox, PJ Gokhale, et al. (2010).

Comparison of defined culture systems for feeder cell free propagation of human embryonic stem cells. In Vitro Cell Dev Biol Anim 46:247–258.
27. Burridge PW, E Matsa, P Shukla, ZC Lin, JM Churko, AD Ebert, F Lan, S Diecke, B Huber, et al. (2014). Chemically defined generation of human cardiomyocytes. Nat Methods 11:855–860.
28. Yokoo N, S Baba, S Kaichi, A Niwa, T Mima, H Doi, S Yamanaka, T Nakahata and T Heike. (2009). The effects of cardioactive drugs on cardiomyocytes derived from human induced pluripotent stem cells. Biochem Biophys Res Commun 387:482–488.
29. Mandel Y, A Weissman, R Schick, L Barad, A Novak, G Meiry, S Goldberg, A Lorber, MR Rosen, J Itskovitz-Eldor and O Binah. (2012). Human embryonic and induced pluripotent stem cell-derived cardiomyocytes exhibit beat rate variability and power-law behavior. Circulation 125:883–893.
30. Davis RP, CW van den Berg, S Casini, SR Braam and CL Mummery. (2011). Pluripotent stem cell models of cardiac disease and their implication for drug discovery and development. Trends Mol Med 17:475–484.
31. Lehnart SE, MJ Ackerman, DW Benson, R Brugada, CE Clancy, JK Donahue, AL George, AO Grant, SC Groft, et al. (2007). Inherited arrhythmias: a National Heart, Lung, and Blood Institute and Office of Rare Diseases workshop consensus report about the diagnosis, phenotyping, molecular mechanisms, and therapeutic approaches for primary cardiomyopathies of gene mutations affecting ion channel function. Circulation 116:2325–2345.
32. Bilet A and CK Bauer. (2012). Effects of the small molecule HERG activator NS1643 on Kv11.3 channels. PLoS One 7:e50886.
33. Girroir EE, HE Hollingshead, AN Billin, TM Willson, GP Robertson, AK Sharma, S Amin, FJ Gonzalez and JM Peters. (2008). Peroxisome proliferator-activated receptor-β/δ (PPARβ/δ) ligands inhibit growth of UACC903 and MCF7 human cancer cell lines. Toxicology 243:236–243.
34. Wu J, HK Jeong, SE Bulin, SW Kwon, JH Park and I Bezprozvanny. (2009). Ginsenosides protect striatal neurons in cellular model of Huntington's disease. J Neurosci Res 87:1904–1912.
35. Mikami D, H Kimura, K Kamiyama, K Torii, K Kasuno, N Takahashi, H Yoshida and M Iwano. (2014). Telmisartan activates endogenous peroxisome proliferator-activated receptor-δ and may have anti-fibrotic effects in human mesangial cells. Hypertens Res 37:422–431.
36. Frydman A. (1992). Pharmacokinetic profile of nicorandil in humans: an overview. J Cardiovasc Pharmacol 20 (Suppl 3):S34–S44.
37. Kobayashi Y, A Miyata, K Tanno, S Kikushima, T Baba and T Katagiri. (1998). Effects of nicorandil, a potassium channel opener, on idiopathic ventricular tachycardia. J Am Coll Cardiol 32:1377–1383.
38. Varothai S and WF Bergfeld. (2014). Androgenetic alopecia: an evidence-based treatment update. Am J Clin Dermatol 15:217–230.
39. Fleishaker JC, NA Andreadis, IR Welshman and CE Wright. (1989). The Pharmacokinetics of 2.5- to 10-mg oral doses of minoxidil in healthy volunteers. J Clin Pharmacol 29:162–167.
40. Joekes AM, FD Thompson and PFB O'Regan. (1981). Clinical use of minoxidil (Loniten). J R Soc Med 74:278–282.
41. Veraitch O, Y Mabuchi, Y Matsuzaki, T Sasaki, H Okuno, A Tsukashima, M Amagai, H Okano and M Ohyama. (2017). Induction of hair follicle dermal papilla cell properties in human induced pluripotent stem cell-derived multipotent LNGFR(+)THY-1(+) mesenchymal cells. Sci Rep 7:42777.
42. Sica DA. (2004). Minoxidil: an underused vasodilator for resistant or severe hypertension. J Clin Hypertens 6:283–287.
43. Mesfin GM, MJ Higgins, FG Robinson and WZ Zhong. (1996). Relationship between serum concentrations, hemodynamic effects, and cardiovascular lesions in dogs treated with minoxidil. Toxicol Appl Pharmacol 140:337–344.
44. Sinnecker D, A Moretti and KL Laugwitz. (2014). Negating the dominant-negative allele: a new treatment paradigm for arrhythmias explored in human induced pluripotent stem cell-derived cardiomyocytes. Eur Heart J 35:1019–1021.
45. Dixon JE, G Osman, GE Morris, H Markides, M Rotherham, Z Bayoussef, AJ El Haj, C Denning and KM Shakesheff. (2016). Highly efficient delivery of functional cargoes by the synergistic effect of GAG binding motifs and cell-penetrating peptides. Proc Natl Acad Sci U S A 113:E291–E299.
46. Fechner H, R Vetter, J Kurreck and W Poller. (2017). Silencing genes in the heart. Methods Mol Biol 1521:17–39.
47. Denning C, V Borgdorff, J Crutchley, KS Firth, V George, S Kalra, A Kondrashov, MD Hoang, D Mosqueira, et al. (2016). Cardiomyocytes from human pluripotent stem cells: from laboratory curiosity to industrial biomedical platform. Biochim Biophys Acta 1863:1728–1748.
48. Colatsky T, B Fermini, G Gintant, JB Pierson, P Sager, Y Sekino, DG Strauss and N Stockbridge. (2016). The Comprehensive in Vitro Proarrhythmia Assay (CiPA) initiative—update on progress. J Pharmacol Toxicol Methods 81:15–20.
49. Liang Y and S Zhao. (2008). Progress in understanding of ginsenoside biosynthesis. Plant Biol (Stuttg) 10:415–421.
50. Zhang LP, YC Jiang, XF Yu, HL Xu, M Li, XZ Zhao and DY Sui. (2016). Ginsenoside Rg3 improves cardiac function after myocardial ischemia/reperfusion via attenuating apoptosis and inflammation. Evid Based Complement Alternat Med 2016:6967853.
51. Choi SH, TJ Shin, BH Lee, DH Chu, H Choe, MK Pyo, SH Hwang, BR Kim, SM Lee, et al. (2010). Ginsenoside Rg3 activates human KCNQ1 K+ channel currents through interacting with the K318 and V319 residues: a role of KCNE1 subunit. Eur J Pharmacol 637:138–147.
52. Choi SH, BH Lee, HJ Kim, SW Jung, HS Kim, HC Shin, JH Lee, HC Kim, H Rhim, et al. (2014). Ginseng gintonin activates the human cardiac delayed rectifier K+ channel: involvement of Ca2+/calmodulin binding sites. Mol Cells 37:656–663.
53. Christ T, A Horvath and T Eschenhagen. (2015). LQT1-phenotypes in hiPSC: are we measuring the right thing? Proc Natl Acad Sci U S A 112:E1968.
54. Greber B, AO Verkerk, G Seebohm, CL Mummery and M Bellin. (2015). Reply to Christ et al.: LQT1 and JLNS phenotypes in hiPSC-derived cardiomyocytes are due to KCNQ1 mutations. Proc Natl Acad Sci U S A 112:E1969.
55. Zhang M, C D'Aniello, AO Verkerk, E Wrobel, S Frank, D Ward-van Oostwaard, I Piccini, C Freund, J Rao, et al. (2014). Recessive cardiac phenotypes in induced pluripotent stem cell models of Jervell and Lange-Nielsen syndrome: disease mechanisms and pharmacological rescue. Proc Natl Acad Sci U S A 111:E5383–E5392.
56. Sala L, Z Yu, D Ward-van Oostwaard, JPD van Veldhoven, A Moretti, KL Laugwitz, CL Mummery, AP Ijzerman and M

Bellin. (2016). A new hERG allosteric modulator rescues genetic and drug-induced long-QT syndrome phenotypes in cardiomyocytes from isogenic pairs of patient induced pluripotent stem cells. EMBO Mol Med 8:1065–1081.
57. Du DT, N Hellen, C Kane and CM Terracciano. (2015). Action potential morphology of human induced pluripotent stem cell-derived cardiomyocytes does not predict cardiac chamber specificity and is dependent on cell density. Biophys J 108:1–4.
58. Rajamohan D, S Kalra, M Duc Hoang, V George, A Staniforth, H Russell, X Yang and C Denning. (2016). Automated electrophysiological and pharmacological evaluation of human pluripotent stem cell-derived cardiomyocytes. Stem Cells Dev 25:439–452.
59. Evans RM, GD Barish and YX Wang. (2004). PPARs and the complex journey to obesity. Nat Med 10:355–361.
60. Miura Y, M Hosono, C Oyamada, H Odai, S Oikawa and K Kondo. (2005). Dietary isohumulones, the bitter components of beer, raise plasma HDL-cholesterol levels and reduce liver cholesterol and triacylglycerol contents similar to PPARalpha activations in C57BL/6 mice. Br J Nutr 93:559–567.
61. Wu X and J Xu. (2016). New role of hispidulin in lipid metabolism: PPARα activator. Lipids 51:1249–1257.
62. Kozako T, S Soeda, M Yoshimitsu, N Arima, A Kuroki, S Hirata, H Tanaka, O Imakyure, N Tone, Si Honda and S Soeda. (2016). Angiotensin II type 1 receptor blocker telmisartan induces apoptosis and autophagy in adult T-cell leukemia cells. FEBS Open Bio 6:442–460.
63. Brunelli L, KA Cieslik, JL Alcorn, M Vatta and A Baldini. (2007). Peroxisome proliferator-activated receptor-delta upregulates 14-3-3 epsilon in human endothelial cells via CCAAT/enhancer binding protein-beta. Circ Res 100:e59–e71.
64. Galuppo M, R Di Paola, E Mazzon, E Esposito, I Paterniti, A Kapoor, C Thiemermann and S Cuzzocrea. (2010). GW0742, a high affinity PPAR-β/δ agonist reduces lung inflammation induced by bleomycin instillation in mice. Int J Immunopathol Pharmacol 23:1033–1046.
65. Yue TL, SS Nerurkar, W Bao, BM Jucker, L Sarov-Blat, K Steplewski, EH Ohlstein and RN Willette. (2008). In vivo activation of peroxisome proliferator-activated receptor-delta protects the heart from ischemia/reperfusion injury in Zucker fatty rats. J Pharmacol Exp Ther 325:466–474.
66. Kim HK, JB Youm, SR Lee, SE Lim, SY Lee, TH Ko, lT Long, B Nilius, dN Won, et al. (2012). The angiotensin receptor blocker and PPAR-γ agonist, telmisartan, delays inactivation of voltage-gated sodium channel in rat heart: novel mechanism of drug action. Pflugers Arch 464:631–643.
67. Ikejima H, T Imanishi, H Tsujioka, A Kuroi, K Kobayashi, M Shiomi, Y Muragaki, S Mochizuki, M Goto, K Yoshida and T Akasaka. (2008). Effects of telmisartan, a unique angiotensin receptor blocker with selective peroxisome proliferator-activated receptor-gamma-modulating activity, on nitric oxide bioavailability and atherosclerotic change. J Hypertens 26:964–972.
68. Batista FAH, DBB Trivella, A Bernardes, J Gratieri, PSL Oliveira, ACM Figueira, P Webb and I Polikarpov. (2012). Structural insights into human peroxisome proliferator activated receptor delta (PPAR-Delta) selective ligand binding. PLoS One 7:e33643.
69. Lee WS and J Kim. (2015). Peroxisome proliferator-activated receptors and the heart: lessons from the past and future directions. PPAR Res 2015:271983.
70. Wu JS, WM Cheung, YS Tsai, YT Chen, WH Fong, HD Tsai, YC Chen, JY Liou, SK Shyue, et al. (2009). Ligand-activated peroxisome proliferator-activated receptor-gamma protects against ischemic cerebral infarction and neuronal apoptosis by 14-3-3 epsilon upregulation. Circulation 119:1124–1134.

Address correspondence to:
Prof. Chris Denning
Department of Stem Cell Biology
Centre of Biomolecular Sciences
University of Nottingham
Nottingham NG7 2RD
United Kingdom

E-mail: chris.denning@nottingham.ac.uk

Received for publication August 15, 2017
Accepted after revision October 9, 2017
Prepublished on Liebert Instant Online October 9, 2017